Received 9 July 2018; revised 18 November 2018; accepted 30 December 2018. Date of publication 15 January 2019; date of current version 25 March 2019.

Digital Object Identifier 10.1109/JPETS.2019.2892418

A Hybrid MMC-Based Photovoltaic and Battery Energy Storage System

HASAN BAYAT[1] (Member, IEEE), AND AMIRNASER YAZDANI[2] (Senior Member, IEEE)

[1]Department of Electrical and Computer Engineering, Western University, London, ON N6A 3K7, Canada
[2]Department of Electrical and Computer Engineering, Ryerson University, Toronto, ON M5B 2K3, Canada

Corresponding author: H. BAYAT (hbayat2@uwo.ca)

ABSTRACT This paper proposes a new configuration and its control strategy for a modular multilevel converter (MMC)-based photovoltaic (PV)-battery energy storage (BES) system. In the MMC-based PV-BES system, each PV submodule is interfaced from its dc side with multiple PV generators using isolated dual active bridge (DAB) dc–dc converters. One BES system is embedded into each arm of the converter and is connected to the dc port of the associated BES submodule using multiple isolated DAB converters. The embedded BES systems are used to smooth the output power of the PV generators and limit the rate of change of the power delivered to the host grid. Moreover, they enable compensation of power mismatches between the arms and legs of the system by exchanging power with the arms of the converter. This paper then proposes a hybrid power mismatch elimination strategy using a combination of power exchange with the arms of the converter and internal power flow control of the MMC. The proposed hybrid power mismatch elimination strategy employs BES systems and differential currents to compensate power mismatches and transfer power between the arms and legs of the converter, respectively. The effectiveness of the proposed power smoothing technique using the embedded BES systems and hybrid power mismatch elimination strategy is demonstrated using time-domain simulations conducted on a switched model of the PV-BES system in PSCAD/EMTDC software environment.

INDEX TERMS Differential current, battery energy storage, control, energy conversion, integration, modular multilevel converter, power electronics, power mismatch, photovoltaic.

I. INTRODUCTION

Photovoltaic solar energy has been growing in a fast pace in the last decade. This growth is associated with concerns about climate change due to the pollution caused by fossil fuel, capital cost reduction of PV panels, and government incentives [1]. As a result, the share of the PV power in the power generation sector is increasing steadily. High penetration of the PV energy resources in the power system poses new challenges which are mainly associated with the intermittent nature of the solar irradiation. The challenges caused by the large-scale PV systems are power quality degradation, stability, and reliability concerns [2]. Output power fluctuations of the PV power plants leads to transients that require large variations in the power output of gas turbines to maintain the balance between power generation and load [3]. This effect translates to frequency regulation challenges. PV power fluctuations can also cause undesirable voltage fluctuations in the distribution level causing flicker and excessive operation of automatic load tap changers of transformers [1].

One approach to resolve the challenges related to the intermittency of the PV power is to curtail the power generation of the PV power plants during cloudy days [3]. This approach is undesirable since it causes substantial loss of revenue. The second approach is using the PV inverters to actively regulate the voltage of the grid at point of common coupling (PCC) by exchanging reactive power with the host grid. This action was explicitly prohibited by the previous version of IEEE 1547 standard. However, the new version of this standard includes voltage and reactive power control requirements [4]. The third approach is to couple the PV power plants with energy storage systems (ESS). The latter approach has the potential to mitigate the aforementioned challenges of the intermittent power resources. Some of the energy storage technologies for renewable power generation applications are pumped hydro [5], super capacitors [6], and batteries [7]. Batteries have gained more attention and application due to scalable power rating [6], lower cost [8], high reliability and efficiency [9], and non-polluting [10].

The main objective of coupling battery energy storage (BES) systems with PV power plants is to smooth the stochastic power output of the PV plants. In the literature, two strategies are proposed to operate the BES system coupled with PV power plants. The first strategy is to operate the PV power plant as a semi-scheduled power generation unit while the second method is to smooth the abrupt changes of the generated PV power. In semi-scheduled mode, a dispatch command, which is based on the projected generation, is received from the operating company and BES systems are used to remove the discrepancies between the actual and projected power generation [6]. In power smoothing mode, battery energy storage system removes the power oscillations of the PV system and limits the ramp rate of the power injected into the grid [3]. Consequently, the power delivered to the host grid becomes smoother with smaller ramp rates.

Modular multilevel converter (MMC)-based PV system is one of the new configurations for integration of utility-scale PV power plants. The MMC-based PV system eliminates bulky grid interface transformers [11], has lower filtering requirements [12], avoids series connection of power switches [13], provides better power quality [14], reduces production costs [15], and improves reliability [16] by virtue of its modularity. The superior performance of the MMC makes it suitable for integration of PV power generators into power system. Reference [17] has proposed the use of MMC to integrate PV generators into a dc grid. MMC as a central converter to integrate a bulk amount of PV power has been proposed in [18]. Application of MMC for EV fleet charging is proposed in [19].

Unequal aggregate power generated by the PV generators connected to the arms of the MMC-based PV system is one of the challenges facing the application of MMC for PV integration. The effect of the aforementioned unequal power generation is injecting unbalanced currents into the grid that can violate the criteria imposed by grid codes and IEEE 1547 standard [20].

The problem of power mismatch between the legs and arms of the MMC-based PV system has been investigated in the literature [21], [22]. Reference [22] proposes adjusting the terminal voltage of the MMC in order to inject balanced currents into the grid whenever a power mismatch happens inside the structure of the MMC-based PV system. Reference [21] proposes using differential currents to eliminate the power mismatches in the MMC-based PV system. However, considering that small fluctuations of the solar irradiation is very common, using the strategy proposed in [21] leads to practically constant presence of differential currents in the structure of the MMC. Consequently, the losses associated with the differential currents increase.

A new structure for the MMC-based PV-BES system is proposed in this paper which embeds one BES in each arm of the converter. Furthermore, a new hybrid power mismatch elimination strategy using a combination of power exchange with the embedded BES systems and internal power flow control of the MMC is proposed in this paper. The fundamental difference between the configuration used in [21] and the configuration proposed in this paper is the presence of BES systems in the arms of the converter. Power exchange between the BES systems and arms of the converter enables the converter to minimize oe nullify power mismatches and the need for transferring power between the legs of the converter.

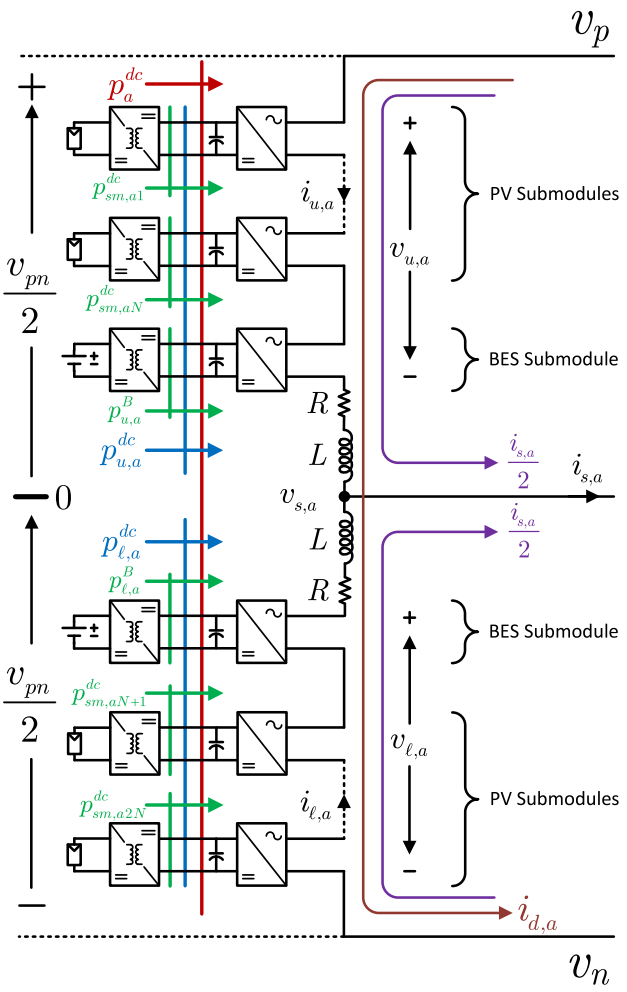

FIGURE 1. **Structure of the MMC-based PV-BES system.**

The proposed hybrid power mismatch elimination strategy uses the embedded BES systems to eliminate power mismatches which are within the power rating of the BES systems and uses a combination of the BES systems and internal power flow control of the MMC to eliminate larger power mismatches. The new structure and its enabling control scheme minimize or mitigate the need for differential currents to eliminate the adverse effects of the PV power fluctuations. The embedded BES systems also are used for smoothing the output power of the MMC-based PV system. Throughout this paper, superscript * denotes the reference value of the corresponding variable.

II. STRUCTURE OF THE MMC-BASED PV-BES SYSTEM

Fig. 1 shows the structure of the proposed MMC-based PV-BES system. Only leg a of the converter is shown to clearly present the details and notation of the converter.

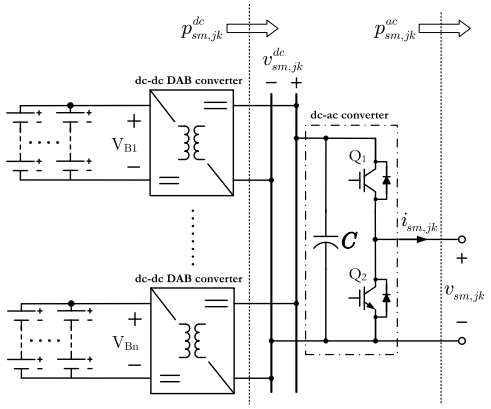

FIGURE 2. Structure of the BES submodules in the hybrid system of Fig. 1.

The proposed MMC configuration consists of three legs, corresponding to three phases of the system, and two arms in each leg, namely upper and lower arms. Each arm of the MMC-based PV-BES system embeds one BES and N PV submodules. Each PV submodule comprises of a half-bridge dc-ac converter, n sets of series- and parallel-connected PV panels (PV generators) with their associated isolated DAB dc-dc converters as presented in [21]. In BES submodules, as shown in Fig. 2, the PV generators of the PV submodule are replaced with battery banks while the rest of the structure remains unaltered. The DAB dc-dc converters are used to interface the PV generators and the battery banks with the dc side of the half-bridge converters.

The isolated dc-dc converters in this paper are considered to be dual active bridge converter (DAB) with medium frequency isolation transformer. The DAB converters interfacing the PV generators are controlled to extract maximum power from the PV generators and the DAB converters interfacing the battery banks are controlled to regulate the power of the battery banks. The galvanic isolation provided by the DAB converters enables the grounding of the negative terminals of the PV generators and eliminates the potential-induced degradation (PID) phenomenon [23].

It should be noted that any dc-dc converter topology featuring galvanic isolation and required power rating could be used instead of the DAB converter. The application of DAB in this paper is due to its galvanic isolation and existing practical implementations of up to 100 kW [24]–[26]. Moreover, for PV submodules, since there is no need for bidirectional power flow, a variant of DAB converter which replaces the secondary bridge with a diode bridge can also be used.

III. POWER SMOOTHING

One of the main objectives of coupling PV farms with storage systems is to smooth the abrupt changes in the output power of the PV generators. The fluctuations of the generated power of PV farms can cause frequency and voltage regulation problems. In this paper, the embedded BES systems are used to smooth the generated power of the PV generators. Simple moving average (SMA) method is applied to determine the amount of power that the BES systems need to absorb or inject in order to limit the rate of change of the power delivered to the host grid. The difference between the aggregate generated power of the PV generators and the output of the SMA is used as the power reference of the BES systems. The reference BES power is divided equally between the BES systems, making them participate equally in limiting the rate of change of the power delivered to the host grid.

The simple moving average is mathematically described as

$$P_{MA}(t) = \frac{1}{m}\sum_{i=1}^{m} P_V(i) \tag{1}$$

where m is the number of samples of the aggregate PV power and P_V is a vector containing the m most recent samples of the aggregate PV power.

The reference power for the BES system of each arm due to the power smoothing function is then defined as

$$P^{BS*}_{u,k}(t) = P^{BS*}_{\ell,k}(t) = \frac{P_{MA}(t) - P_{PV}(t)}{6} \quad k = a, b, c \tag{2}$$

where $P^{BS}_{u,k}(t)$ and $P^{BS}_{\ell,k}(t)$ are the powers for the BES systems of the upper and lower arm of leg k due to power smoothing function, respectively. Since all BES systems are assigned the same amount of power by the power smoothing function, they will not change the amount of power mismatches.

IV. PROPOSED HYBRID POWER MISMATCH ELIMINATION STRATEGY AND ITS ENABLING SCHEMES

The final goal of the PV-BES system of Fig. 1 is to extract the maximum power from the PV generators and inject it into the host grid using balanced three-phase currents. Meaning that, one third of the aggregate power of the PV generators will be injected into the grid from each phase of the converter.

The proposed MMC configuration and its enabling control strategy ensures that the goal of equal power injection into the host grid is achieved with minimum differential current in the structure of the MMC. Upon occurrence of a power mismatch, a power management strategy uses the embedded BES systems to eliminate the power mismatch. If the power mismatch is within the power rating of the embedded BES systems, the power mismatch will be eliminated without creating differential currents.

The different types of power mismatch that can happen in the structure of the MMC-based PV-BES system of Fig. 1 are:

1) Power mismatch between the legs of the converter described mathematically as

$$p^{dc}_a(t) \neq p^{dc}_b(t) \neq p^{dc}_c(t) \tag{3}$$

where $p^{dc}_k(t)$ is the aggregate power delivered by the PV generators to leg k.

2) Power mismatch between the arms of leg k

$$p^{dc}_{u,k}(t) \neq p^{dc}_{\ell,k}(t) \tag{4}$$

where $p^{dc}_{u,k}(t)$ and $p^{dc}_{\ell,k}(t)$ are the aggregate power delivered by the PV generators to the upper and lower arms of leg k, respectively.

3) Power mismatch between the submodules of one arm

The first and second types of power mismatches stated above are the topic of this paper. The third item is automatically manged using the voltage sorting algorithm in voltage balancing technique [21] .

A. ELIMINATION OF SMALL LEG AND ARM POWER MISMATCHES

One objective of embedding BES systems in the arms of the MMC-based PV system is to equalize the aggregate power of the legs of the converter. Defining the average leg power as

$$p_{av}(t) = \frac{1}{3}\sum_{k=a,b,c} p^{dc}_{k}(t) \qquad k = a, b, c \tag{5}$$

The equalized power of the legs can be written as

$$p_{av}(t) = p^{dc}_{k}(t) + p^{BM*}_{u,k}(t) + p^{BM*}_{\ell,k}(t) \tag{6}$$

where $P^{BM}_{u,k}$ and $P^{BM}_{\ell,k}$ are the power of the BES systems of the upper and lower arms of leg k due to power mismatch elimination function, respectively. If the condition shown in (6) is met, dc differential currents are not needed to eliminate the leg power mismatches.

Sum of the powers of the BES systems of the upper and lower arms for leg k is derived from (6) as

$$p^{BM*}_{u,k}(t) + p^{BM*}_{\ell,k}(t) = p_{av}(t) - p^{dc}_{k}(t) \tag{7}$$

The next objective of embedding BES systems in the arms of the MMC-based PV system is to equalize the aggregate power between the arms of leg k which is formulated as

$$p^{dc}_{u,k}(t) + p^{BM*}_{u,k}(t) = p^{dc}_{\ell,k}(t) + p^{BM*}_{\ell,k}(t) \tag{8}$$

The difference between the powers of the BES of the upper and lower arms for leg k is derived from (8) as

$$p^{BM*}_{u,k}(t) - p^{BM*}_{\ell,k}(t) = p^{dc}_{\ell,k}(t) - p^{dc}_{u,k}(t) \tag{9}$$

Solving the system of linear equations consisting of (7) and (9) yields the power setpoint for each BES in the MMC due to power mismatch function as

$$\begin{aligned} p^{BM*}_{u,k}(t) &= \frac{p_{av}(t)}{2} - p^{dc}_{u,k}(t) \\ p^{BM*}_{\ell,k}(t) &= \frac{p_{av}(t)}{2} - p^{dc}_{\ell,k}(t) \end{aligned} \tag{10}$$

Having generated the reference powers for the BES of each arm due to power smoothing scheme using (2) and due to the power mismatch elimination strategy using (10), the two quantities are added to yield the final power setpoint for each BES as

$$\begin{aligned} P^{B*}_{u,k}(t) &= P^{BS*}_{u,k}(t) + P^{BM*}_{u,k}(t) \\ P^{B*}_{\ell,k}(t) &= P^{BS*}_{\ell,k}(t) + P^{BM*}_{\ell,k}(t) \end{aligned} \tag{11}$$

The power setpoints of the BES systems, calculated using (11), correspond to a condition which the existing power mismatch can be eliminated using the BES systems and differential currents are not needed. However, if the powers calculated in (11) are outside the power capability of the BES systems, a differential current will be created to transfer power between the arms and legs of the converter. As a result, the values calculated in (11) have to be examined to determine if they are within the power capabilities of the BES systems. Fig. 3 shows the process to examine the reference power of each BES system. Where P^{B*} represents the power setpoint for any given BES system.

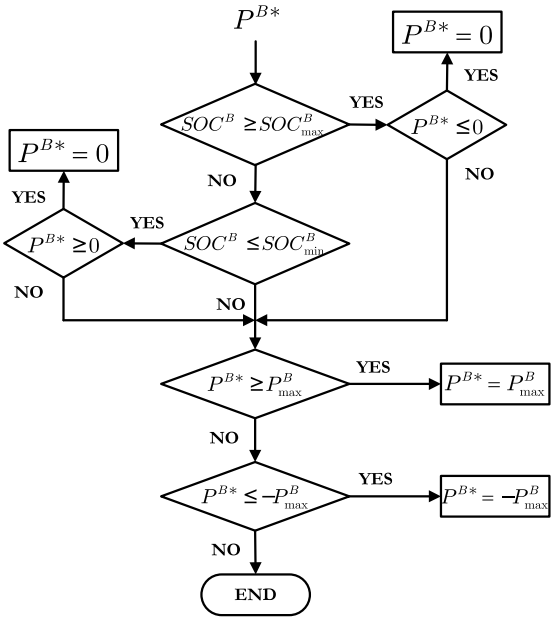

FIGURE 3. Flowchart to evaluate the power reference of the BES systems.

B. ELIMINATION OF LARGE LEG POWER MISMATCHES

The ultimate goal of the proposed MMC-based PV-BES system is to inject equal powers from each phase of the MMC into grid while keeping the differential current at minimum. This goal can be represented mathematically as

$$\underbrace{p^{dc}_{u,k} + p^{dc}_{\ell,k}}_{p^{dc}_{k}} + p^{B}_{u,k} + p^{B}_{\ell,k} + p^{ex}_{k} = p_{av} \tag{12}$$

where $p^{ex}_{k}(t)$ is the term that needs to be added to the aggregate generated power of the PV generators and BES systems of leg k to equalize the powers injected into the grid by each phase. The term is referred as the *power mismatch* of leg k which reflects the power mismatch between the aggregate generated power of the PV generators of the legs including the BES systems.

Equation (12) can be rewritten as

$$p^{ex}_{k}(t) = p_{av}(t) - p^{dc}_{k}(t) - p^{B}_{u,k}(t) - p^{B}_{\ell,k}(t) \tag{13}$$

After defining the amount of power mismatch of each leg, $p^{ex}_{k}(t)$, the setpoint for the dc differential currents of each

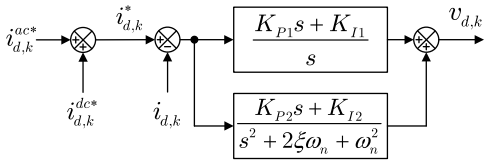

FIGURE 4. Block diagram of the scheme for controlling the differential currents.

leg is calculated as

$$i_{d,k}^{dc*}(t) = \frac{p_k^{ex}(t)}{v_{pn}} \quad k = a, b, c \tag{14}$$

where $i_{d,k}^{dc}(t)$ is the dc component of the differential current of leg k. The term v_{pn} is the voltage between the positive and negative rails of the MMC. Equation (14) indicates that the dc differential currents sum up to zero at the positive and negative rails of the MMC.

C. ELIMINATION OF LARGE ARM POWER MISMATCHES

The goal of the arm power mismatch elimination strategy is to eliminate the power mismatches between the arms of each leg using embedded battery energy storage systems. The goal is reached by exchanging power between the embedded BES systems and their associated arms to equalize the aggregate power of the arms of each leg. Having calculated the power reference of the BES system of each arm, the flowchart shown in Fig. 3 is used to evaluate the power rating limitation of the storage systems and adjust the calculated values of BES power setpoints. Then, the adjusted power references are used to define the amount of power that needs to be transferred between the arms of each leg according to

$$p_{d,k}(t) = p_{u,k}^{dc}(t) + p_{u,k}^{B}(t) - p_{\ell,k}^{dc}(t) - p_{\ell,k}^{B}(t) \tag{15}$$

where $p_{d,k}(t)$ is the differential power of leg k including the powers of its BES systems. Having defined the differential power of each leg in (15), the $\alpha\beta$-frame values of the ac differential currents are calculated according to the procedure outlined in [21] and are used to generate the ac components of the three-phase differential current commands in abc-frame, $i_{d,k}^{ac*}(t)$.

The final commands for the differential currents are determined using the dc and ac differential current commands as

$$i_{d,k}^{*} = i_{d,k}^{dc*} + i_{d,k}^{ac*} \tag{16}$$

where $i_{d,k}$ is the differential component of the arm current in leg k. Having generated the final commands for the differential currents using (16), the differential current controller (DCC) shown in Fig. 4 is used to generate the currents in the legs of the MMC.

Fig. 5 shows a higher-level depiction of the controller of the converter which relates all the controller components.

V. SIMULATION RESULTS

The MMC-based PV-BES system of Fig. 1 is simulated in PSCAD/EMTDC software environment. The simulation results demonstrate the effectiveness of the proposed hybrid power mismatch elimination strategy in minimizing/eliminating the need for differential currents to mitigate the power mismatches between the arms and legs of the MMC system. To allow faster simulations, the DAB converters are represented by controllable current sources and the half-bridge converters are represented by their switched model. The simulated PV-BES system has 9 PV submodules ($N = 9$), and 1 BES submodule in each arm. The power rating of the PV and BES submodules is 100 kW. The dc link voltage reference of the submodules is set to 0.8 kV. Also, to keep the simulation model tractable, one DAB converter and one PV generator model are used in each submodule (i.e., $n = 1$).

The PV generators consists of 3 parallel-connected strings of 23 series-connected panels of Kyocera KU330-8BCA. Each PV panel generates 330 W under standard testing condition (STC). The DAB converters interfacing the PV generators with the dc side of the half-bridge converters exercise the perturb and observe (P&O) MPPT algorithm. The battery banks consist of 64 batteries of IND27-2V Trojan Battery Company which are configured into strings of 16 batteries to reach the voltage rating of 768 V and 4 such strings are connected in parallel to reach the energy capacity of 97.23 kAh. Series resistance of the battery bank is considered to be 0.2 ohm. The grid voltage is 4.16 kV (line-to-line, rms). Table 1 lists the other parameters of the simulated system.

A. CASE 1: POWER SMOOTHING

One of the applications of the BES systems coupled with PV farms is to smooth the abrupt changes of the output power of the PV farms. The proposed MMC-based PV-BES system is capable of smoothing the generated power of the PV generators by exchanging power with the arms of the system. SMA is used to determine the amount of the power that BES systems need to exchange with each arm in order to reduce the overall power fluctuations of the injected power into the host grid. Simple moving average has been calculated for duration of 1/2 min with 1/2 s sampling rate, resulting in averaging of the 60 most recent samples. The difference between the output of the SMA algorithm and the actual aggregate power of the PV generators is used as the power reference for the BES systems. In this scenario, all the BES systems are assigned the same power reference. The solar irradiation data has been extracted from [27].

Fig. 6(a) shows the solar irradiation of the PV generators. Initially the PV generators are all subjected to solar irradiation of 900 W/m^2. Then at t = 5 s, the solar irradiation undergoes intermittent changes due to partial cloud coverage of the PV generators. The aggregate power injected into the grid and the power generated by the PV generators are shown in Fig. 6(b). As confirmed by Fig. 6(b), the power injected

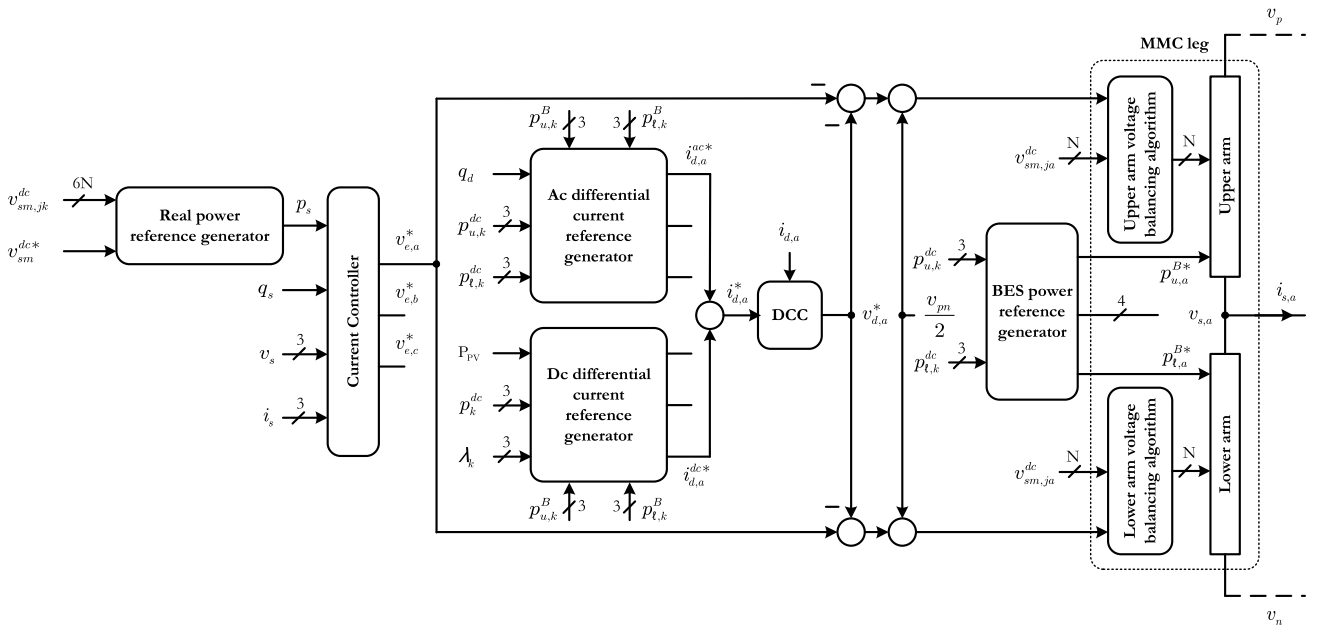

FIGURE 5. Top-level block diagram of the controller of the MMC-based PV-BES system.

TABLE 1. Parameters of the MMC and grid.

Parameter	Value	Parameter	Value
L	3 mH	K_{P1}	3
R	0.1 Ω	K_{I1}	100
L_g	750 μH	K_{P2}	100
R_g	60 $m\Omega$	K_{I2}	1
C	10 mF	SOC^B_{min}	10%
ζ	0.05	SOC^B_{max}	90%
ω_n	$2\pi\times60$	P^B_{max}	100 kW

into the grid is smoother than the aggregate power generated by the PV generators. Fig. 6(c) shows the aggregate power of the BES systems which is positive or negative during discharging and charging intervals, respectively. The time intervals that the BES systems absorb power from the arms of the MMC (charging batteries) are shown as green patches and the time intervals that the BES systems inject power into the arms of the MMC (discharging batteries) are shown in red patches. One of the advantages of the simple moving average is that at the end of the day the batteries will have the same state of charge (SOC) they had at the end of the previous day.

B. CASE 2: ARM AND LEG POWER MISMATCH ELIMINATION

This case demonstrates the performance of the proposed MMC-based PV-BES system and its control strategy in presence of power mismatches between the arms and legs of the converter. Thus, initially the PV generators are all subjected to STC (solar irradiation 1000 W/m^2 and temperature 25°C). Then, at t = 0.05 s, the solar irradiation of the PV generators of the upper arm of leg a is decreased gradually to 900 W/m^2, which results in the generated power decline as

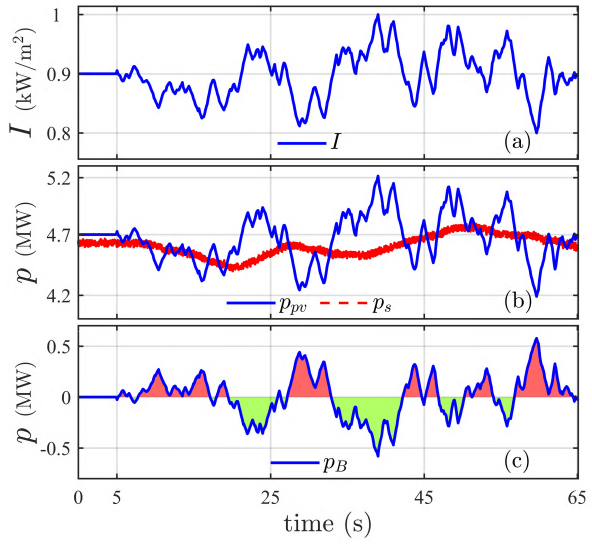

FIGURE 6. Response to power smoothing (case 1).

shown in Fig. 7(a). This irradiation change translates to leg power mismatch and 90 kW arm power mismatch in leg a. However, since the power mismatch is less than the power rating of the embedded BES systems, the power mismatch is mitigated by exchanging power with the BES systems, as illustrated in Figs. 7(d) through 7(f). As shown in Fig. 7(b), at t = 0.1 s, the power of the PV generators connected to the upper arm of leg b is decreased from 0.87 MW to 0.7 MW. This power mismatch grows beyond power rating of the BES systems at t = 0.26 s where the BES of the upper arm of leg b reaches its power limit, as shown in 8(e). As a result, a differential current is created in the system to transfer power between the arms and legs of the converter as

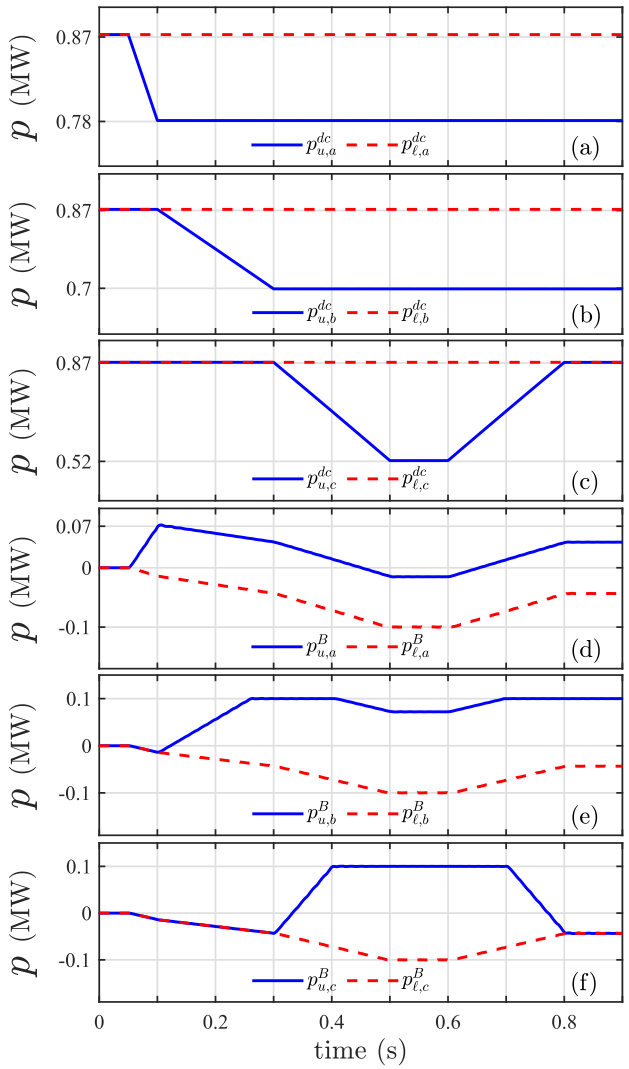

FIGURE 7. **Response to power mismatch (case 2).**

shown in Figs. 8(a)-8(c). Between t = 0.05 s and t = 0.26 s, the existing power mismatches are mitigated using the embedded BES systems without the need for differential currents.

At t = 0.3 s, the solar irradiation of the PV generators of the upper arm of leg *c* is declined causing their generated power to decrease from 0.87 MW to 0.52 MW. At t = 0.6 s the change is reversed to evaluate the performance of the proposed structure and controller when the power mismatch returns within the power rating of the BES systems. Fig. 7(c) shows the power generated by the PV generators of the arms of leg *c*. As shown in Figs. 7(f), the power of the BES system of the upper arm of leg *c* increases upon initiation of the power mismatch and after reaching its maximum power, a differential current is created to transfer power between arms and legs of the converter as shown in Figs. 8(a) through 8(c). At t = 0.7 s, where the generated power of the PV generators of the upper arm in leg *c* increases, the differential current becomes smaller while the remaining power mismatch is eliminated by the embedded BES systems.

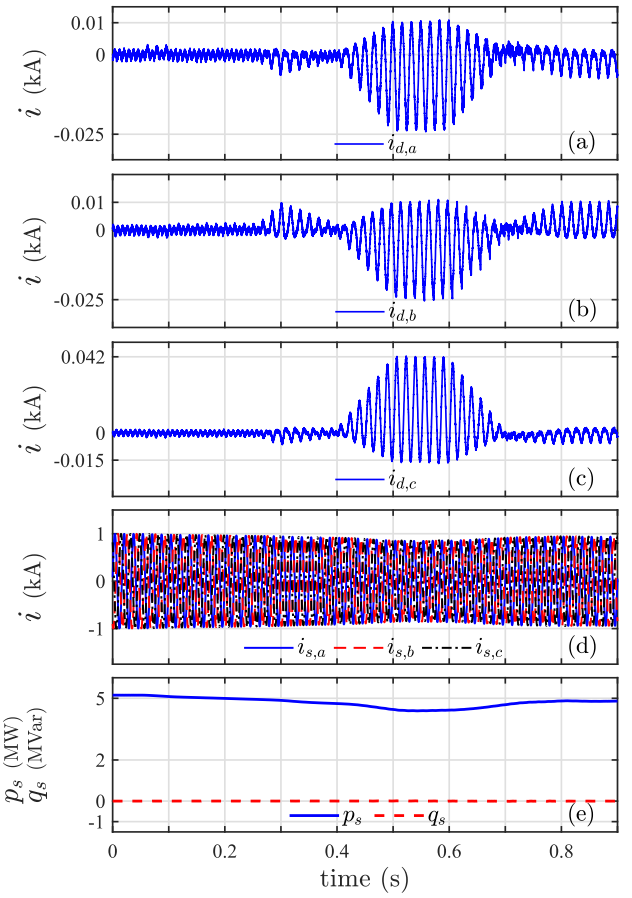

FIGURE 8. **Response to power mismatch (case 2).**

Fig. 8(d) shows the current injected into the grid which remains balanced and symmetrical in spite of the existing power mismatches in the MMC-based PV-BES system. The real and reactive power exchanged between the MMC-based PV-BES system and the host grid is shown in Fig. 8(e). Reactive power remains regulated at its reference, which is zero, and active power is regulated by the current controller to keep the balance between the generated PV power and the power injected into the grid.

C. CASE 3: SIMULTANEOUS POWER SMOOTHING AND POWER MISMATCH ELIMINATION

The PV generators are initially subjected to solar irradiation of 800 W/m^2. Then, at t = 1 s, the solar irradiation of the PV generators is switched to an intermittent irradiation causing their output power to fluctuate, as shown in Figs. 9(a)-9(c). At t = 4 s, the solar irradiation of the PV generators of the upper arm of leg *b* is decreased by 100 W/m^2 which corresponds to arm and leg power mismatches while the solar irradiation fluctuates intermittently. The embedded BES systems react to the power mismatches and eliminate the power mismatches by exchanging power with their corresponding arms, as shown in Figs. 9(d)-9(f). At *t* = 7 s, the solar irradiation of the PV generators of the upper arm of leg *c* is reduced by 300 W/m^2. The arm and leg power mismatches

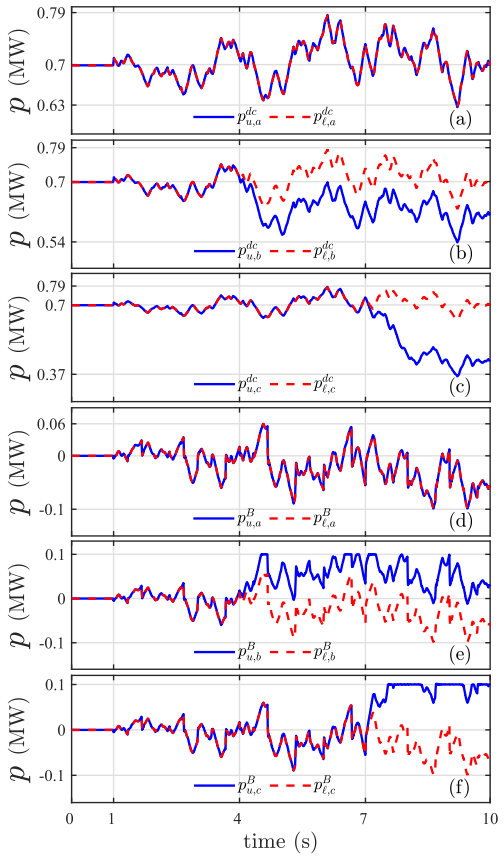

FIGURE 9. Response to simultaneous power smoothing and power mismatch (case 3).

caused by this irradiation decline fall outside the power rating of the BES systems, as inferred from Figs. 9(e)-9(f). Consequently, differential currents are created inside the structure of the MMC, as shown in Fig. 10(a)-10(c), that transfer power between the arms and legs of the converter. Fig. 10(d) shows the real and reactive powers exchanged between the MMC-based PV-BES system and the host grid. The reactive power follows its reference and remains at zero while the real power changes smoothly according to the output of the SMA algorithm.

VI. CONCLUSION

A new structure and power mismatch elimination strategy for a medium-voltage PV-BES system is proposed in this paper. The proposed PV-BES system employs a modular multilevel converter (MMC) of which the PV submodules are interfaced with PV generators using multiple dc-dc dual active bridge (DAB) converters enabling independent maximum power point tracking (MPPT) and grounding of the PV generators. The battery energy storage (BES) submodules are embedded into the structure of the MMC system where each arm hosts a BES submodule. The BES submodules are interfaced with the battery banks using a dc-dc DAB converter which controls the amount of power exchange with the batteries. The proposed hybrid power mismatch

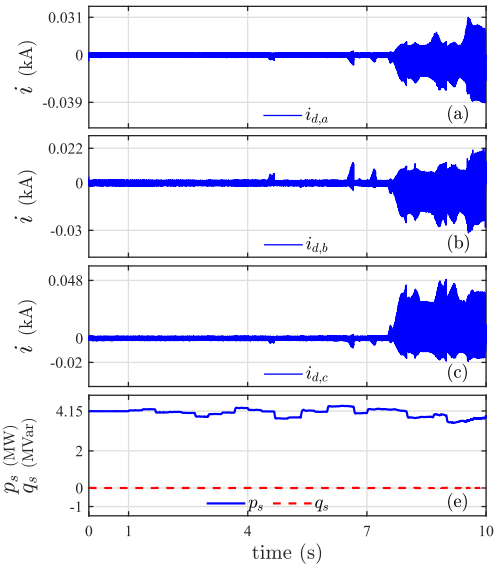

FIGURE 10. Response to simultaneous power smoothing and power mismatch (case 3).

elimination strategy utilizes the power exchange capability with the embedded BES systems to eliminate small power mismatches without creating differential currents. Moreover, for large power mismatches, the proposed hybrid power mismatch elimination strategy employs the power exchange with embedded BES systems and internal power flow control of the MMC to mitigate the power mismatch with minimum differential current. The proposed power mismatch elimination strategy ensures that one third of the generated PV power is injected into the host grid from each phase of the converter and also keeps the injected currents balanced in despite of unequal PV power generation in each leg of the converter. The embedded storage systems also are used to smooth the output power of the PV system and limit the rate of change of the power delivered to the grid. The effectiveness of the proposed power mismatch elimination strategy is demonstrated by time-domain simulations conducted on a representative model of the system in PSCAD/EMTDC environment.

REFERENCES

[1] G. K. Ari and Y. Baghzouz, "Impact of high PV penetration on voltage regulation in electrical distribution systems," in *Proc. Int. Conf. Clean Electr. Power (ICCEP)*, Jun. 2011, pp. 744–748.

[2] S. Vazquez, S. M. Lukic, E. Galvan, L. G. Franquelo, and J. M. Carrasco, "Energy storage systems for transport and grid applications," *IEEE Trans. Ind. Electron.*, vol. 57, no. 12, pp. 3881–3895, Dec. 2010.

[3] Y. Moumouni, Y. Baghzouz, and R. F. Boehm, "Power 'smoothing' of a commercial-size photovoltaic system by an energy storage system," in *Proc. 16th Int. Conf. Harmon. Quality Power (ICHQP)*, May 2014, pp. 640–644.

[4] *IEEE Standard for Interconnection and Interoperability of Distributed Energy Resources With Associated Electric Power Systems Interfaces*, IEEE Standard 1547-2018 (Revision IEEE Std 1547-2003), Apr. 2018, pp. 1–138.

[5] R. Jiang, J. Wang, and Y. Guan, "Robust unit commitment with wind power and pumped storage hydro," *IEEE Trans. Power Syst.*, vol. 27, no. 2, pp. 800–810, May 2012.

[6] G. Wang, M. Ciobotaru, and V. G. Agelidis, "Power smoothing of large solar PV plant using hybrid energy storage," *IEEE Trans. Sustain. Energy*, vol. 5, no. 3, pp. 834–842, Jul. 2014.

[7] H. Beltran, E. Bilbao, E. Belenguer, I. Etxeberria-Otadui, and P. Rodriguez, "Evaluation of storage energy requirements for constant production in PV power plants," *IEEE Trans. Ind. Electron.*, vol. 60, no. 3, pp. 1225–1234, Mar. 2013.
[8] P. F. Ribeiro, B. K. Johnson, M. L. Crow, A. Arsoy, and Y. Liu, "Energy storage systems for advanced power applications," *Proc. IEEE*, vol. 89, no. 12, pp. 1744–1756, Dec. 2001.
[9] H. Chen, T. N. Cong, W. Yang, C. Tan, Y. Li, and Y. Ding, "Progress in electrical energy storage system: A critical review," *Prog. Natural Sci.*, vol. 19, no. 3, pp. 291–312, 2009.
[10] S. C. Smith, P. K. Sen, and B. Kroposki, "Advancement of energy storage devices and applications in electrical power system," in *Proc. IEEE Power Energy Soc. General Meeting–Convers. Del. Electr. Energy 21st Century*, Jul. 2008, pp. 1–8.
[11] M. Glinka and R. Marquardt, "A new AC/AC-multilevel converter family applied to a single-phase converter," in *Proc. 5th Int. Conf. Power Electron. Drive Syst. (PEDS)*, vol. 1, Nov. 2003, pp. 16–23.
[12] U. N. Gnanarathna, A. M. Gole, and R. P. Jayasinghe, "Efficient modeling of modular multilevel HVDC converters (MMC) on electromagnetic transient simulation programs," *IEEE Trans. Power Del.*, vol. 26, no. 1, pp. 316–324, Jan. 2011.
[13] S. Debnath, J. Qin, B. Bahrani, M. Saeedifard, and P. Barbosa, "Operation, control, and applications of the modular multilevel converter: A review," *IEEE Trans. Power Electron.*, vol. 30, no. 1, pp. 37–53, Jan. 2015.
[14] F. Deng and Z. Chen, "A control method for voltage balancing in modular multilevel converters," *IEEE Trans. Power Electron.*, vol. 29, no. 1, pp. 66–76, Jan. 2014.
[15] K. Wang, Y. Li, and Z. Zheng, "Voltage balancing control and experiments of a novel modular multilevel converter," in *Proc. IEEE Energy Convers. Congr. Expo. (ECCE)*, Sep. 2010, pp. 3691–3696.
[16] G. Casadei, R. Teodorescu, C. Vlad, and L. Zarri, "Analysis of dynamic behavior of modular multilevel converters: Modeling and control," in *Proc. 16th Int. Conf. Syst. Theory, Control Comput. (ICSTCC)*, Oct. 2012, pp. 1–6.
[17] J. Echeverria, S. Kouro, M. Perez, and H. Abu-Rub, "Multi-modular cascaded DC-DC converter for HVDC grid connection of large-scale photovoltaic power systems," in *Proc. 39th Annu. Conf. Ind. Electron. Soc. (IECON)*, Nov. 2013, pp. 6999–7005.
[18] M. Alsadah and F. Mancilla-David, "Modeling and control of grid-connected photovoltaic power plants utilizing a simplified model of the modular multilevel converter," in *Proc. North Amer. Power Symp. (NAPS)*, Sep. 2014, pp. 1–6.
[19] M. Mao *et al.*, "Multi-objective power management for EV fleet with MMC-based integration into smart grid," *IEEE Trans. Smart Grid*, to be published, doi: 10.1109/TSG.2017.2766363.
[20] *IEEE Standard for Interconnecting Distributed Resources With Electric Power Systems*, IEEE Standard 1547.2-2008, Apr. 2009, pp. 1–217.
[21] H. Bayat and A. Yazdani, "A power mismatch elimination strategy for an MMC-based photovoltaic system," *IEEE Trans. Energy Convers.*, vol. 33, no. 3, pp. 1519–1528, Sep. 2018.
[22] S. Rivera, B. Wu, R. Lizana, S. Kouro, M. Perez, and J. Rodriguez, "Modular multilevel converter for large-scale multistring photovoltaic energy conversion system," in *Proc. IEEE Energy Convers. Congr. Expo. (ECCE)*, Sep. 2013, pp. 1941–1946.
[23] S. Pingel *et al.*, "Potential induced degradation of solar cells and panels," in *Proc. 35th IEEE Photovoltaic Specialists Conf.*, Jun. 2010, pp. 2817–2822.
[24] M. N. Kheraluwala, R. W. Gascoigne, D. M. Divan, and E. D. Baumann, "Performance characterization of a high-power dual active bridge DC-to-DC converter," *IEEE Trans. Ind. Appl.*, vol. 28, no. 6, pp. 1294–1301, Nov./Dec. 1992.
[25] R. T. Naayagi, A. J. Forsyth, and R. Shuttleworth, "Bidirectional control of a dual active bridge dc-dc converter for aerospace applications," *IET Power Electron.*, vol. 5, no. 7, pp. 1104–1118, Aug. 2012.
[26] H. Akagi, S. I. Kinouchi, and Y. Miyazaki, "Bidirectional isolated dual-active-bridge (DAB) DC-DC converters using 1.2-kV 400-A SiC-MOSFET dual modules," *CPSS Trans. Power Electron. Appl.*, vol. 1, no. 1, pp. 33–40, Dec. 2016.
[27] J. Marcos, L. Marroyo, E. Lorenzo, and M. García, "Smoothing of PV power fluctuations by geographical dispersion," *Progr. Photovoltaics, Res. Appl.*, vol. 20, no. 2, pp. 226–237, 2012, doi: 10.1002/pip.1127.

HASAN BAYAT (S'15–M'18) received the B.Sc. degree from Guilan University, Rasht, Iran, in 2008, the M.Sc. degree from the Amirkabir University of Technology, Tehran, Iran, in 2009, and the Ph.D. degree from Western University (formerly, The University of Western Ontario), London, ON, Canada, in 2018, all in electrical engineering. His research interests include renewable electric power systems, control and modeling of electronic power converters, and energy storage systems.

AMIRNASER YAZDANI (M'05–SM'09) received the Ph.D. degree in electrical engineering from the University of Toronto, Toronto, ON, Canada, in 2005. He is currently a Professor at Ryerson University, Toronto. His research interests include the modeling and control of electronic power converters, renewable electric power systems, distributed generation and storage, and microgrids.